Porosity-enhanced solar powered hydrogen generation in GaN photoelectrodes

Y. Hou, Z. Ahmed Syed, L. Jiu, J. Bai, and T. Wang

Articles you may be interested in

Porosity-enhanced solar powered hydrogen generation in GaN photoelectrodes

Y. Hou, Z. Ahmed Syed, L. Jiu, J. Bai, and T. Wang[a)]
Department of Electronic and Electrical Engineering, University of Sheffield, Mappin Street, Sheffield S1 3JD, United Kingdom

Two types of GaN based photoelectrodes using either horizontally aligned or vertically aligned nanopores have been fabricated by means of using an electrochemical etching approach. The photoelectrodes based on such nanostructures have demonstrated an up to 5-fold enhancement in applied bias photon-to-current efficiency and incident photon-to-current efficiency in comparison with their planar counterpart, leading to a high Faradaic conversion efficiency which approaches 1. The GaN photoelectrodes with these nanopores also show excellent chemical stability in HBr solution as an electrolyte. The results presented reveal that the gas diffusion in the nanopores plays an important role in water splitting processes, which should be taken into account when designing a GaN photoelectrode with a nanopore structure. © 2017 Author(s). All article content, except where otherwise noted, is licensed under a Creative Commons Attribution (CC BY) license (http://creativecommons.org/licenses/by/4.0/). https://doi.org/10.1063/1.5001938

Solar powered hydrogen generation based on a photoelectrochemical (PEC) mechanism has been attracting considerable attention since the 1970s,[1] as it involves a simple process which can directly convert solar energy into clean and storable energy in the form of hydrogen. III-nitrides have been regarded as one of the most promising material systems for such an application due to a number of major advantages. For example, GaN exhibits excellent chemical stability in either acidic or alkaline solution, where solar powered hydrogen generation can be performed efficiently. Furthermore, the band structure of GaN can straddle over the redox potential of water (1.23 eV), which is essential for performing an overall water splitting reaction.[2] However, the energy conversion efficiency of GaN-based photoelectrodes reported so far is far too low, typically less than $0.1 \, \text{mA/cm}^2$ in photocurrent density obtained under AM1.5 1 Sun illumination.[3–5] It is well-known that the carrier diffusion length of GaN is ∼200 nm. Consequently, it is expected that GaN nanostructures with a physical dimension of less than 200 nm can potentially lead to a significant enhancement in solar to hydrogen (STH) conversion efficiency.[6–17]

Nanoporous GaN may be one of the very promising nanostructures utilised for solar powered hydrogen generation,[16] as nanoporous GaN provides a number of advantages in terms of enhanced surface-to-volume ratio and reduced carrier travelling distance, maximising the chance for energetic electrons/holes participating in both the oxygen-evolution half-reaction and the hydrogen-evolution half-reaction before their recombination.

Electrochemical (EC) etching is emerging as a simple but effective approach to the fabrication of nanoporous GaN for a wide range of applications.[18–21,23,24] The EC etching approach was first introduced to the fabrication of porous Si and then was transferred to the conventional III-V semiconductors such

as InP for optoelectronic applications.[22] It is worth highlighting that this approach is particularly important for chemically inert GaN because it is very difficult to perform standard chemical etching on GaN. Although there is increasing interest in applying nanoporous GaN in fabricating optoelectronics such as laser diodes including vertical cavity surface emitting lasers (VCSELs) and light emitting diodes,[18–21,23,24] there are only a few reports on solar powered hydrogen generation so far. Very recently, we have demonstrated a significant enhancement in STH efficiency using a GaN photoelectrode with nanopores, which was fabricated using a photo-assisted electrochemical etching approach. In this case, the nanopores exhibit a random distribution in terms of size and orientation.[15]

The mechanism of EC etching without involving any illumination, which is different from the photo-assisted electrochemical etching mentioned above, is based on a combination of an oxidation process and then a dissolution process in acidic solution under an anodic bias.[25] Under a positive anodic bias, the injection of holes leads to the oxidation of GaN, and the oxidized layer is then chemically dissolved in an acidic electrolyte. Therefore, EC etching can be performed on n-type GaN with good conductivity only. Otherwise, holes which are necessary for the generation of the oxidation process cannot be provided. Note that if the applied bias is too high or the doping concentration of n-type GaN is too high, the whole layer may be etched away, and thus, nanoporous GaN cannot be formed either.[26]

In theory, if the direction of injection current can be controlled, GaN nanopores can be fabricated along any particular direction desired. In this paper, we have reported two kinds of GaN photoelectrodes with nanopores fabricated under different conditions, where the nanopores orient along either the vertical direction or the horizontal direction. Both devices demonstrate different behaviours in solar powered water splitting although both devices show significantly enhanced conversion efficiency compared to their planar

a)Author to whom correspondence should be addressed: t.wang@sheffield.ac.uk

counterparts. The GaN electrode with vertically aligned nanopores exhibits superior performance to that with horizontally aligned nanopores.

Generally speaking, there exist two major approaches for the fabrication of GaN nanostructures, for instance, nanowire growth by molecular beam epitaxial (MBE) or metal-organic chemical vapour deposition (MOCVD)[15,16] and post-growth fabrication of nanostructures utilised in the present work. The major advantage of our GaN nanopores fabricated using the EC approach is due to the fact that the diameter and orientation of nanopores can be simply controlled through the doping level and applied bias.[25,26] Furthermore, such nanopores can be filled with other materials such as dye or colloidal quantum dots with long absorption wavelengths, further enhancing the performance. Moreover, the prototype nanoporous GaN devices demonstrated in this work can be easily extended to other III-nitrides such as InGaN which can cover the whole solar spectrum.

All the photoelectrodes used in the present work are fabricated from a standard n-type GaN wafer grown on (0001) sapphire by metal-organic chemical vapour deposition (MOCVD) using our high temperature AlN buffer technique.[27] After depositing an initial AlN buffer layer and then a 300 nm nominally un-doped GaN layer, a Si doped n-type GaN layer with a thickness of about 1.2 μm was grown. The carrier concentration and mobility of the n-GaN layer are $1.8 \times 10^{19}/cm^3$ and 191 cm^2/V s, respectively, which are determined at room temperature by the standard van der Pauw method. The wafer is diced into a number of pieces of samples each with a rectangular shape ($0.5 \times 2 \, cm^2$) for further photoelectrode fabrication.

All the nanoporous GaN as photoelectrodes have been fabricated using the above n-type GaN samples by means of an EC etching method. The EC etching is carried out in acidic solution using a Keithley 2401 as a potentiostat. Note that there is no UV light illumination involved in the EC etching processes, which is different from the photo-assisted electrochemical etching approach. The n-GaN samples with an indium contact are used as an anode, while a Pt wire is used as a counter electrode. Scanning electron microscopy (SEM) measurements are conducted using a Raith SEM system.

For solar powered hydrogen generation measurements, a copper wire is bonded onto an indium ohmic contact using silver epoxy. The whole contact area is covered by insulating epoxy for protection as usual. A Pt wire is used as a counter electrode. The illumination source employed is an LOT-Orial solar simulator equipped with a 300 W ozone-free Xe lamp. 1 M HBr is used as an electrolyte for all the solar powered hydrogen generation measurements. The same Keithley 2401 is used as a source meter.

In order to fabricate nanoporous GaN along the vertical direction, an indium contact is made on a small corner of the top surface of each piece of the n-GaN sample; the rest surface can be exposed to an electrolyte during the EC etching process, and thus, the etching process will proceed from the top vertically downwards. The sample with vertically aligned nanopores is fabricated in 0.5 M HNO_3 (pH = 0.3) under a bias of 20 V for 30 min without any UV light illumination. We monitor that the etching current drops to a base line level, meaning that the n-GaN layer has been etched into nanoporous GaN.

Figure 1(a) shows a cross-sectional SEM image, indicating that the vertically aligned nanopores exhibit a diameter of around 40 nm. In addition, there is a very thin un-etched layer just below the top surface. The formation of this very thin un-etched layer is due to a kind of "depletion region" formed at the interface between n-GaN and the electrolyte (similar to a p-n junction), where the thin layer is highly resistant and thus cannot be etched away. This thin un-etched layer can be chemically etched away under UV-light illumination whose energy is higher than the bandgap of GaN, where holes can be generated as a result of optical excitation. The photo-generated holes then oxidize the thin
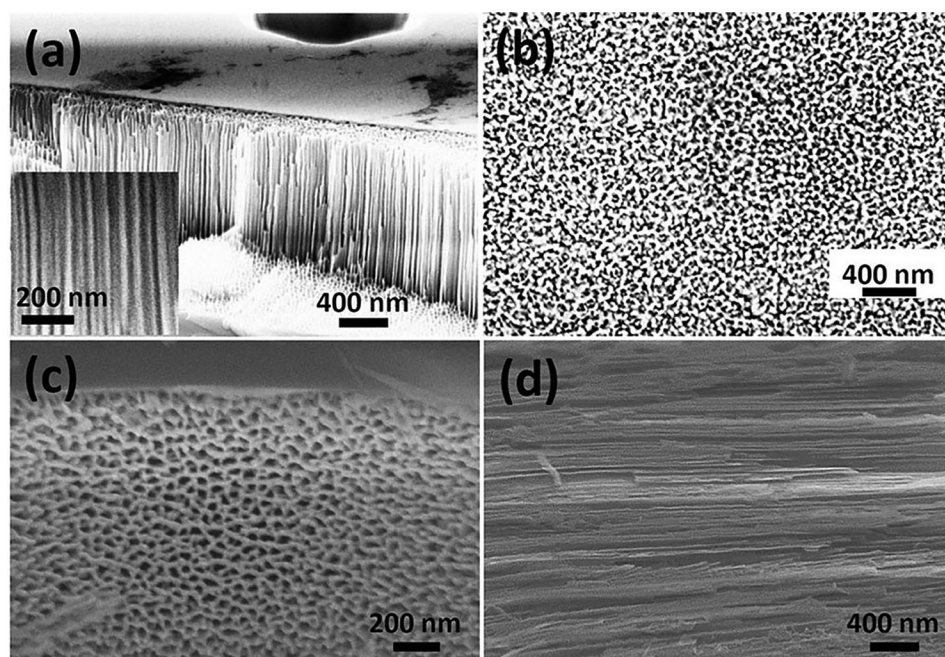

FIG. 1. Cross-sectional SEM image (a) and plan-view image (b) of the sample with vertically aligned nanopores; Cross-sectional SEM image (c) and plan-view image (d) of the sample with horizontally aligned nanopores.

resistant "depletion" region, and this thin oxidised layer is finally dissolved in the chemical solution.

Figure 1(b) shows a plan-view SEM image of the GaN nanopores after the thin un-etched layer is removed by UV-assisted electrochemical etching performed using a low bias of 6 V under 500 W Xe lamp illumination in 0.35 M KOH for 10 minutes. From Fig. 1(b), the porosity is estimated to be $>2.5 \times 10^{10}/cm^2$, leading to a significantly increased surface area by a factor of more than 37 times compared to its planar counterpart. Note that the morphology of the nanopores is not affected even though the electrolyte concentration is further increased up to 1 M. However, with decreasing applied bias, the size of the nanopores decreases along with the increasing thickness of sidewalls. If the applied bias is further reduced down to 5 V, there is no EC etching observed, which is similar to other reports.[20,25]

In order to fabricate horizontally aligned nanopores, an injection current needs to flow along the horizontal direction. For this purpose, the surface of the n-GaN sample is covered by a 200 nm SiO_2 layer deposited by using plasma-assisted chemical vapour deposition (PECVD), but leaving a small corner of the top surface of an n-GaN sample uncovered (where an indium contact is made). Subsequently, a number of parallel trenches with a period of 2000 μm are fabricated (defined by photolithography and then dry etching). The trenches will be exposed to an electrolyte during an EC etching process. As a result of SiO_2 which is insulating, the EC etching process will proceed along the horizontal direction.

Figure 1(c) displays a cross-sectional SEM image, confirming that the horizontally aligned nanopores have been formed under identical EC conditions (i.e., 0.5 M HNO_3 for 30 min at 20 V). The nanopores have a diameter of 40–60 nm and a density of $\sim 2.8 \times 10^{10}/cm^2$. Figure 1(d) shows that the nanopores are formed through the whole regions between two adjacent trenches which are 2000 μm apart.

Both the vertically aligned nanopores and the horizontally aligned nanopores do not exhibit difference in terms of the diameter of nanopores because the diameter is mainly determined by either doping concentration or applied bias.[25,26]

For simplicity, the devices with vertically aligned nanopores or horizontally aligned nanopores are labelled as Device **A** and Device **B**, respectively. Prior to any solar powered hydrogen generation experiments, a plasma treatment is implemented in order to passivate the samples, aiming to further enhance chemical stability and lifetime. The samples are first cleaned in H_2SO_4 (98%):H_2O (1:1) solution to remove any potential contaminates generated during the nanoporous fabrication processes. The samples are exposed to RF irradiation with 80 W for 20 min under flowing SF_6 with a flow rate of 30 standard cubic centimetres (scc) per minute, as sulphite can effectively passivate III-nitrides.[28] Fluorine radicals are expected to remove any potential oxides formed during the EC fabrication process. Finally, a copper wire is soldered onto the indium ohmic contact, and the whole contact is fully covered with insulating epoxy. 1 M HBr is used an electrolyte. The solar power used is 100 mW/cm^2, i.e., 1 Sun under AM1.5 conditions.

Figure 2(a) shows the photocurrent density of the devices as a function of applied potential ranging from −1.5 to 1.8 V (vs. Ag/AgCl as a reference electrode), where the
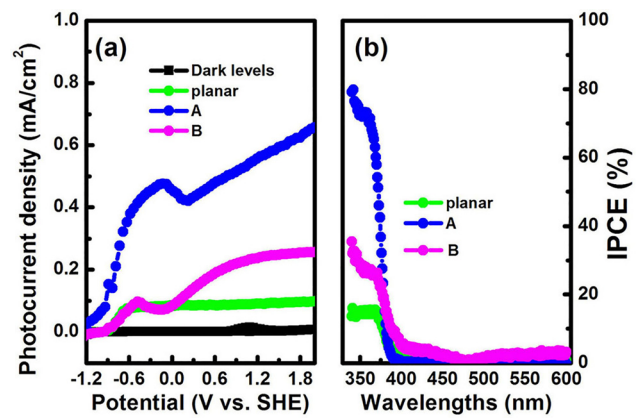

FIG. 2. (a) Photocurrent density as a function of applied potential against Ag/AgCl as a reference electrode; (b) IPCE as a function of wavelength measured under an applied bias of 0.8 V.

measured potentials vs. Ag/AgCl have been converted to the reversible hydrogen electrode (RHE) scale according to the Nernst equation[9]

$$V_{RHE} = V_{Ag/AgCl} + 0.059 \times pH + V^0_{Ag/AgCl}, \quad (1)$$

where $V^0_{Ag/AgCl} = 0.197$ V.

Figure 2(a) shows that the planar photoelectrode as a reference exhibits only ~ 0.1 mA/cm^2, which is a typical value observed in the previous work,[3–5,17] while a 6-fold enhancement in photocurrent density has been obtained for Device **A** compared to the reference. For Device **B**, only a 2-fold enhancement in photocurrent density has been observed compared to the reference.

Applied bias photon-to-current efficiency (ABPE), which is generally defined below, has also been measured on all the devices.

$$ABPE = \frac{J(mA\,cm^{-2}) \times (1.23 - V_b)}{P(mW\,cm^{-2})} \times 100\%, \quad (2)$$

where J is the photocurrent density measured under an applied bias V_b and P is the incident solar power density.

Under an applied bias of 0.8 V, the ABPE values of Devices **A** and **B** are 0.3% and 0.13%, respectively, while the ABPE of the reference planar photoelectrode is only 0.06% measured under identical conditions.

Incident photon-to-current conversion efficiency (IPCE) measurements have been performed on all the devices in 1 M HBr at an applied bias of 0.8 V under 75 W Xe lamp illumination. The incident power has been calibrated using a Si enhanced photodetector. The expression of IPCE is given below,

$$IPCE = \frac{1240 \times J(mA\,cm^{-2})}{\lambda(nm) \times P(mW\,cm^{-2})} \times 100\%, \quad (3)$$

where J, λ, and P are the photocurrent density, the wavelength, and the incident power density, respectively.

Figure 2(b) shows the IPCE as a function of wavelength, demonstrating that an IPCE of 73% has been achieved on Device **A** at around 360 nm, (i.e., at the band-edge of GaN). This is much higher than the IPCE of Device **B** (31%). For

comparison purposes, the IPCE of the reference photoelectrode is only 15%. Clearly, the enhanced ABPE and IPCE can be attributed to the increased ratio of surface-area to volume as a result of the nanopores. This also indicates that the GaN photoelectrode with vertically aligned nanopores is more efficient.

Device **B** exhibits much lower IPCE than Device **A**. In order to understand the physics behind this phenomenon, electrochemical impedance spectra (EIS) have been measured on these devices under dark conditions using a function generator (Digimess FG100) which can provide signals with a frequency ranging from 100 to 1 M Hz and a dual-trace oscilloscope (Hitachi V422).

Figure 3 shows the EIS of all the devices typically expressed in a Nyquist plot,[9,29] where the inset provides an equivalent circuit diagram. C_{se}, R_{se}, and R_s are the differential capacitance across the semiconductor-electrolyte interface, the resistance of the photocathode or the electrolyte resistance, and the resistance at the semiconductor−electrolyte interface, respectively.

Generally speaking, the semicircle in a Nyquist plot at high frequencies describes the charge transfer process, and the diameter of the semicircle is equal to the charge transfer resistance. Figure 3 shows that the planar photoelectrode exhibits the largest impedance among all the devices, while the GaN photoelectrodes with either vertical aligned nanopores or horizontally aligned nanopores have a reduced impedance by a factor of ~1.6–3, demonstrating an enhanced charge transfer. The reduced impedance can be attributed to the fact that the dimension of our GaN nanopores is far less than the carrier diffusion length of GaN (about 200 nm).

Consequently, the difference in both photocurrent density and IPCE between Devices **A** and **B** might be attributed to gaseous diffusion. For Device **B**, it is likely that the generated oxygen on the working electrode cannot efficiently escape from the nanopores due to their configuration. As a result, the gaseous oxygen may accumulate at the interface between the electrolyte and GaN, slowing down water splitting reactions. It is plausible that the oxygen generated in Device **A** (i.e., with vertically aligned nanopores) experiences a shorter distance to escape from the nanopores than that in Device **B**. (i.e., with horizontally aligned nanopores).
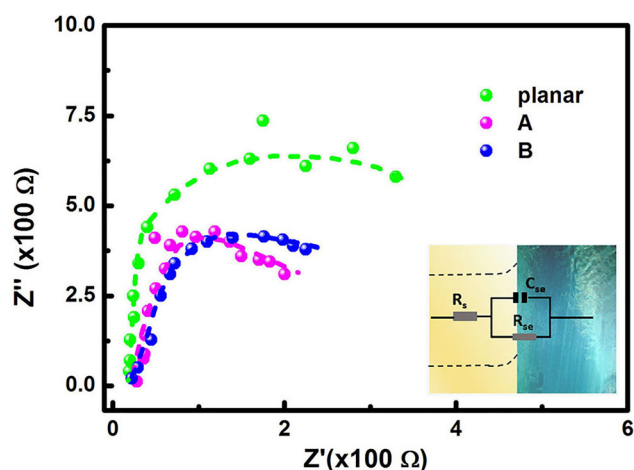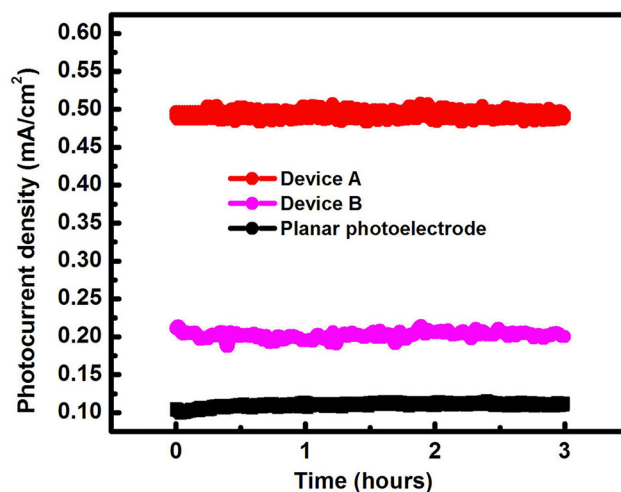
FIG. 4. Photocurrent density as a function of time tested under continuous 100 mW/cm^2 illumination at 0.8 V in 1 M HBr for 3 h for Device **A**, Device **B**, and the reference planar device.

The chemical stability of our devices with nanopores has been studied. For example, Fig. 4 shows the photocurrent densities of Device **A** and Device **B** (and the reference planar device) as a function of time tested under continuous 100 mW/cm^2 illumination at 0.8 V for 3 h, demonstrating that there is no degradation in photocurrent density for both our devices with nanopores and the planar device. Finally, 0.15 ml of H_2 has been collected from the counter electrode for Device **A**, indicating a Faradaic efficiency approaching 1. This also further confirms a great enhancement in the STH efficiency of Device **A** compared to that of the reference planar device.

We have reported two kinds of GaN photoelectrodes with either vertically aligned or horizontally aligned nanopores. They are fabricated by means of using an EC etching approach under different conditions. Detailed solar powered hydrogen generation experiments including ABPE and IPCE have been performed, demonstrating a significant enhancement in photocurrent density compared to their planar counterpart. Electrochemical impedance spectra have also been measured, indicating lower impedance for the devices with nanopores than their planar counterpart. It is worth highlighting that the device with vertically aligned nanopores exhibits much superior performance to the device with horizontally aligned nanopores GaN. Furthermore, both devices with nanopores exhibit excellent stability in HBr solution as an electrolyte. Our results presented could potentially pave the way for the fabrication of a high-efficiency hybrid photoelectrode based on III-nitrides.

FIG. 3. EIS of all the devices drawn in a Nyquist plot. Inset: Equivalent circuit diagram.

[1]A. Fujishima and K. Honda, Nature **238**, 37–38 (1972).
[2]P. G. Moses and C. G. Van de Walle, Appl. Phys. Lett. **96**, 021908 (2010).
[3]J. Benton, J. Bai, and T. Wang, Appl. Phys. Lett. **103**, 133904 (2013).
[4]Y. Hou, Z. A. Syed, R. Smith, M. Athanasiou, Y. Gong, J. Bai, and T. Wang, J. Phys. D: Appl. Phys. **49**, 265601 (2016).
[5]J. Benton, J. Bai, and T. Wang, Appl. Phys. Lett. **102**, 173905 (2013).

[6]B. Liu, R. Smith, J. Bai, Y. Gong, and T. Wang, Appl. Phys. Lett. **103**, 101108 (2013).

[7]M. Ebaid, J. H. Kang, S. H. Lim, Y. H. Cho, and S. W. Ryu, RSC Adv. **5**, 23303 (2015).

[8]N. u H. Alvi, P. E. D. S. Rodriguez, P. Aseev, V. J. Gómez, A. u H. Alvi, W. u. Hassan, M. Willander, and R. Nötzel, Nano Energy **13**, 291 (2015).

[9]P. Varadhan, H. C. Fu, D. Priante, J. R. D. Rentamal, C. Zhao, M. Ebaid, T. K. Ng, I. Ajia, S. Mitra, I. S. Roqan, B. S. Ooi, and J. H. He, Nano Lett. **17**, 1520 (2017).

[10]Y. J. Hwang, C. H. Wu, C. Hahn, H. E. Jeong, and P. Yang, Nano Lett. **12**, 1678–1682 (2012).

[11]B. AlOtaibi, H. P. T. Nguyen, S. Zhao, M. G. Kibria, S. Fan, and Z. Mi, Nano Lett. **13**, 4356 (2013).

[12]T. Tao, T. Zhi, B. Liu, M. Li, Z. Zhuang, J. Dai, Y. Li, F. Jiang, W. Luo, Z. Xie, D. Chen, P. Chen, Z. Li, Z. Zou, R. Zhang, and Y. Zheng, Sci. Rep. **6**, 20218 (2016).

[13]S. Fan, S. Y. Woo, S. Vanka, G. A. Botton, and Z. Mi, APL Mater. **4**, 076106 (2016).

[14]C. Pendyala, J. B. Jasinski, J. H. Kim, V. K. Vendra, S. Lisenkov, M. Menon, and M. K. Sunkara, Nanoscale **4**, 6269–6275 (2012).

[15]Y. Hou, X. Yu, Z. A. Syed, S. Shen, J. Bai, and T. Wang, Nanotechnology **27**, 455401 (2016).

[16]B. AlOtaibi, M. Harati, S. Fan, S. Zhao, H. P. T. Nguyen, M. G. Kibria, and Z. Mi, Nanotechnology **24**, 175401 (2013).

[17]J. Benton, J. Bai, and T. Wang, Appl. Phys. Lett. **105**, 223902 (2014).

[18]Y. Zhang, S. W. Ryu, C. Yerino, B. Leung, Q. Sun, Q. Song, H. Cao, and J. Han, Phys. Status Solidi B **247**, 1713–1716 (2010).

[19]D. Cao, H. Xiao, J. Fang, J. Liu, Q. Gao, X. Liu, and J. Ma, Mater. Res. Express **4**, 015019 (2017).

[20]C. Yang, L. Liu, S. Zhu, Z. Yu, X. Xi, S. Wu, H. Cao, J. Li, and L. Zhao, J. Phys. Chem. C **121**, 7331–7336 (2017).

[21]G. Yuan, K. Xiong, C. Zhang, Y. Li, and J. Han, ACS Photonics **3**, 1604 (2016).

[22]G. Su, Q. Guo, and R. E. Palmer, J. Appl. Phys. **94**, 7598 (2003).

[23]G. Y. Shiu, K. T. Chen, F. H. Fan, K. P. Huang, W. J. Hsu, J. J. Dai, C. F. Lai, and C. F. Lin, Sci. Rep. **6**, 29138 (2016).

[24]T. Braniste, J. Ciers, E. Monaico, D. Martin, J.-F. Carlin, V. V. Ursaki, V. V. Sergentu, I. M. Tiginyanu, and N. Grandjean, Superlattices Microstruct. **102**, 221 (2017).

[25]M. J. Schwab, D. Chen, J. Han, and L. D. Pfefferle, J. Phys. Chem. C **117**, 16890 (2013).

[26]C. Zhang, S. H. Park, D. Chen, D. W. Lin, W. Xiong, H. C. Kuo, C. F. Lin, H. Cao, and J. Han, ACS Photonics **2**, 980 (2015).

[27]T. Wang, J. Bai, P. J. Parbrook, and A. G. Cullis, Appl. Phys. Lett. **87**, 151906 (2005).

[28]C. Zhao, T. K. Ng, A. Prabaswara, M. Conroy, S. Jahangir, T. Frost, J. O'Connell, J. D. Holmes, P. J. Parbrook, P. Bhattacharya, and B. S. Ooi, Nanoscale **7**, 16658 (2015).

[29]M. Ebaid, J. H. Kang, and S. W. Yu, J. Electrochem. Soc. **162**, H264–H270 (2015).